npj | vaccines

Article

Published in partnership with the Sealy Institute for Vaccine Sciences

https://doi.org/10.1038/s41541-025-01135-8

Controlling reactogenicity while preserving immunogenicity from a self-amplifying RNA vaccine by modulating nucleocytoplasmic transport

Jason A. Wojcechowskyj ✉, Robyn M. Jong, Imre Mäger, Britta Flach, Paul V. Munson, Progya P. Mukherjee, Barbara Mertins, Katherine R. Barcay & Thomas Folliard ✉

Self-amplifying RNA (saRNA)-based vaccines have emerged as a potent and durable RNA vaccine platform relative to first generation mRNA vaccines. However, RNA vaccine platforms trigger undesirable side effects at protective doses, underscoring the need for improved tolerability. To address this, we leveraged the Cardiovirus leader protein, which is well-characterized to dampen host innate signaling by modulating nucleocytoplasmic transport (NCT). Co-administration of a leader-protein-encoding mRNA (which we have named "RNAx") delivered alongside vaccine cargo saRNA reduced interferon production while enhancing Influenza hemagglutinin (HA) expression in human primary cells and murine models. RNAx potently decreased serum biomarkers of reactogenicity after immunizations with an HA-expressing saRNA-LNP vaccine while maintaining the magnitude of the antibody and cellular response. RNAx also consistently enhanced binding antibody titers after a single injection and in some conditions enhanced binding antibody and neutralization titers post-boost. These findings support RNAx as a promising platform approach for improving tolerability of saRNA-LNP vaccines while preserving or enhancing immunogenicity.

RNA lipid nanoparticle (LNP) vaccines represent a breakthrough in vaccinology, offering unprecedented speed in responding to emerging pathogens while providing robust protection and simplified manufacturing[1]. However, despite the public health success of SARS-CoV-2 mRNA-LNP vaccines, these vaccines exhibit undesirable side effects at protective μg doses levels[2] and are expensive to manufacture rapidly on a global scale[3]. Self-amplifying RNA (saRNA) vaccines are compelling alternatives to conventional mRNA platforms, providing longer lasting protection at lower μg doses[4–6]. The higher potency per μg dose from saRNA is likely a product of both robust antigen expression and higher levels of adjuvancy arising from innate signaling, inherent to the saRNA platform. Self-replication in a cell generates double-stranded RNA (dsRNA) intermediates, a potent adjuvant that itself can contribute to systemic reactogenicity[7–9]. While innate pathways provide crucial adjuvant effects, their overactivation can trigger reactogenicity and suppress immune responses from RNA-based vaccines, for example, by inhibiting antigen expression. saRNA and dsRNA are potent inducers of primary interferons (IFN-α/β), which have been shown to inhibit both T cell[10,11] and B cell responses[12–15] from RNA vaccines.

Significant research has been conducted to balance saRNA-induced innate signaling with vaccine efficacy. One set of strategies has been to modify the intrinsic potency of the saRNA molecule itself, which facilitates dose sparing and thus reduces reactogenicity[6,16]. Others have deployed orthogonal lipid-based delivery modalities that are less reactogenic than LNPs[13,17,18]. Based on the enabling success of using modified uridine nucleosides with mRNA-based vaccines[19–22], recent efforts have uncovered a different modified nucleoside, 5-methylcytosine (5mC), that partially reduces saRNA-induced innate signaling and reactogenicity[23,24]. Lastly, another strategy is to target excessive innate signaling directly either through co-administering small molecule inhibitors[12,25] or by co-expressing protein-based inhibitors of innate signaling[12,26]. While these approaches show considerable promise, there remains an opportunity to develop a universal strategy that combines low μg doses with effective suppression of saRNA-induced reactogenicity.

Here we report the engineering of the leader protein from Cardiovirus, a genus of RNA viruses from the Picornaviridae family that broadly dampens excessive innate immune activation triggered by saRNA. The leader

ExcepGen Inc. Emeryville, San Francisco, CA, USA. ✉e-mail: jwojcechowskyj@gmail.com; thomas.folliard@excepgen.com

protein inhibits innate signaling and interferon (IFN) production[27] driven by the IRF-3 transcription factor[28] and disrupts translational inhibition induced by PKR activation[29] through interference with nucleocytoplasmic transport (NCT)[30–33]. This mechanism of suppressing host gene expression is essential for viral gene expression and replication in IFN-competent hosts[34,35]. We leveraged this function of the leader protein to balance excessive saRNA-driven innate signaling and IFN production in the context of an saRNA vaccine. Here, we encode the leader protein from a small mRNA termed "RNAx". A key advantage of RNAx is that it targets NCT broadly, thus enabling suppression of diverse innate signaling pathways simultaneously[36].

From experiments in cell lines, primary human immune cells, and mouse models, we find that RNAx suppresses saRNA-induced IFN production and other proinflammatory cytokines while enhancing antigen expression both in vitro and in vivo. We also find that RNAx enhances gene of interest (GOI) expression and suppresses proinflammatory cytokines from unmodified mRNA-LNPs in mice. Following administration of an saRNA-LNP vaccine in mice, higher doses of RNAx potently suppress biomarkers of systemic reactogenicity while preserving the cellular and antibody response. At lower doses of RNAx, the antibody response was consistently enhanced after a single injection and occasionally following the boost. These findings establish RNAx as a modular and tunable platform technology for reducing reactogenicity while maintaining immunogenicity or in some contexts improving the antibody response of saRNA vaccines. The modular nature of encoding RNAx from a discrete mRNA unlocks the potential of improving any RNA-based vaccine, with the ability to fine tune dose for better tolerability and/or dose-sparing enabled by increases in potency.

Results

RNAx enhances GOI expression from saRNA

RNAx, derived from the Cardiovirus leader protein, suppresses antiviral innate signaling[28] and PKR-mediated inhibition of translation[29], thereby enhancing viral gene expression[34,35] (Fig. 1A). We first combined RNAx with saRNA in two different forms: either as a single RNA molecule under the control of an internal ribosome entry site (IRES), "*in cis*", or as a discrete mRNA, "in trans" (Fig. 1B). Using a strain of the Venezuelan equine encephalitis virus (VEEV) Simplicon vector, we cloned three reporter constructs under the control of the subgenomic promoter with RNAx *in cis* to estimate the impact on GOI expression: Influenza hemagglutinin (HA) fused at the C-terminus with nano-Luciferase (HA-nLuc), a secreted form of nLuc (sec-nLuc), and firefly luciferase (fLuc). We transfected these reporter constructs with or without RNAx *in cis* into BJ cells, a normal human diploid fibroblast cell line previously utilized for studying the impact of innate signaling on GOI expression from RNA[37]. Relative to saRNA only, saRNA with RNAx *in cis* enhanced the expression of HA-nLuc 62-fold, sec-nLuc 34-fold, and fLuc 8-fold (Fig. 1C). As a control for potential changes to the ability of IRES-containing constructs to express GOI, we also transfected 293 T cells, which lack robust expression of innate sensors of dsRNA[19,38]. Each of the constructs expressed similar levels of reporter protein regardless of the presence of RNAx in 293 T cells, consistent with a model where RNAx dampens intact innate signaling (Fig. 1C). When RNAx was co-transfected

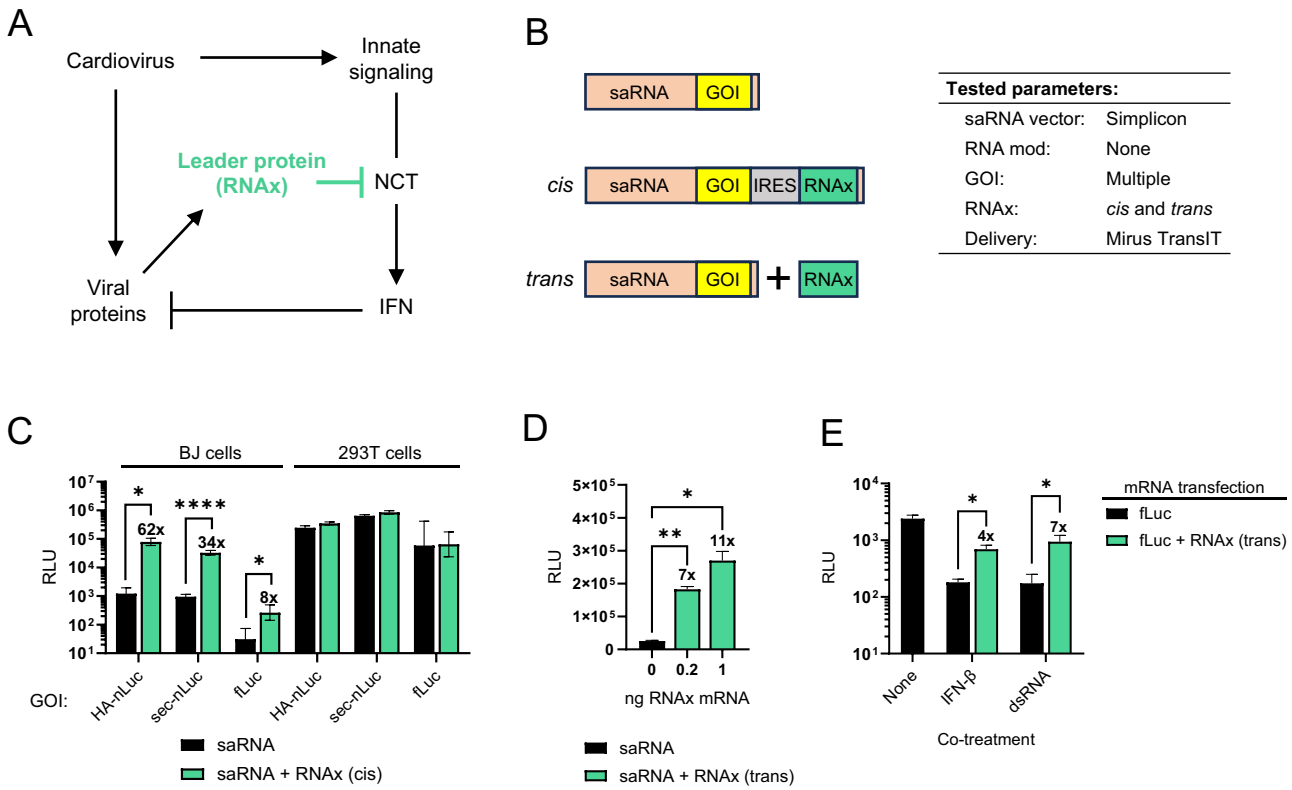

Fig. 1 | RNAx enhances GOI expression from saRNA in vitro. A The Cardiovirus leader protein suppresses innate signaling by dampening nucleocytoplasmic transport (NCT) in infected cells. RNAx refers to an mRNA that encodes for the leader protein. **B** RNAx was expressed from VEEV saRNA in cis from an IRES downstream of GOI or added in trans from a modified nucleoside mRNA. **C** RNAx enhances GOI expression in cells with intact innate signaling. BJ or 293 T cells were transfected with reporter constructs and Luc signal measured 48 h later with or without RNAx in cis. **D** RNAx enhances GOI expression in a dose-responsive fashion in trans. BJ cells were transfected with secreting nLuc-expressing saRNA with increasing amounts of RNAx in trans and 6 days post transfection supernatants were harvested for nLuc activity. **E** RNAx reverses suppression of mRNA reporter activity in the presence of IFN-β or dsRNA (Poly I:C). BJ cells were transfected with a modified nucleoside fLuc-encoding mRNA and co-treated with either 1 ng/mL recombinant IFN-β or 100 ng/mL Poly(I:C). Luc activity was measured 48 h post transfection from cell lysates. Mean ± SEM, $n = 3–4$. $^{*}p < 0.05$, $^{**}p < 0.01$, $^{****}p < 0.0001$ Ratio paired t-test. Numbers above bars indicate average fold change enhancement of RNAx containing groups relative to no RNAx.

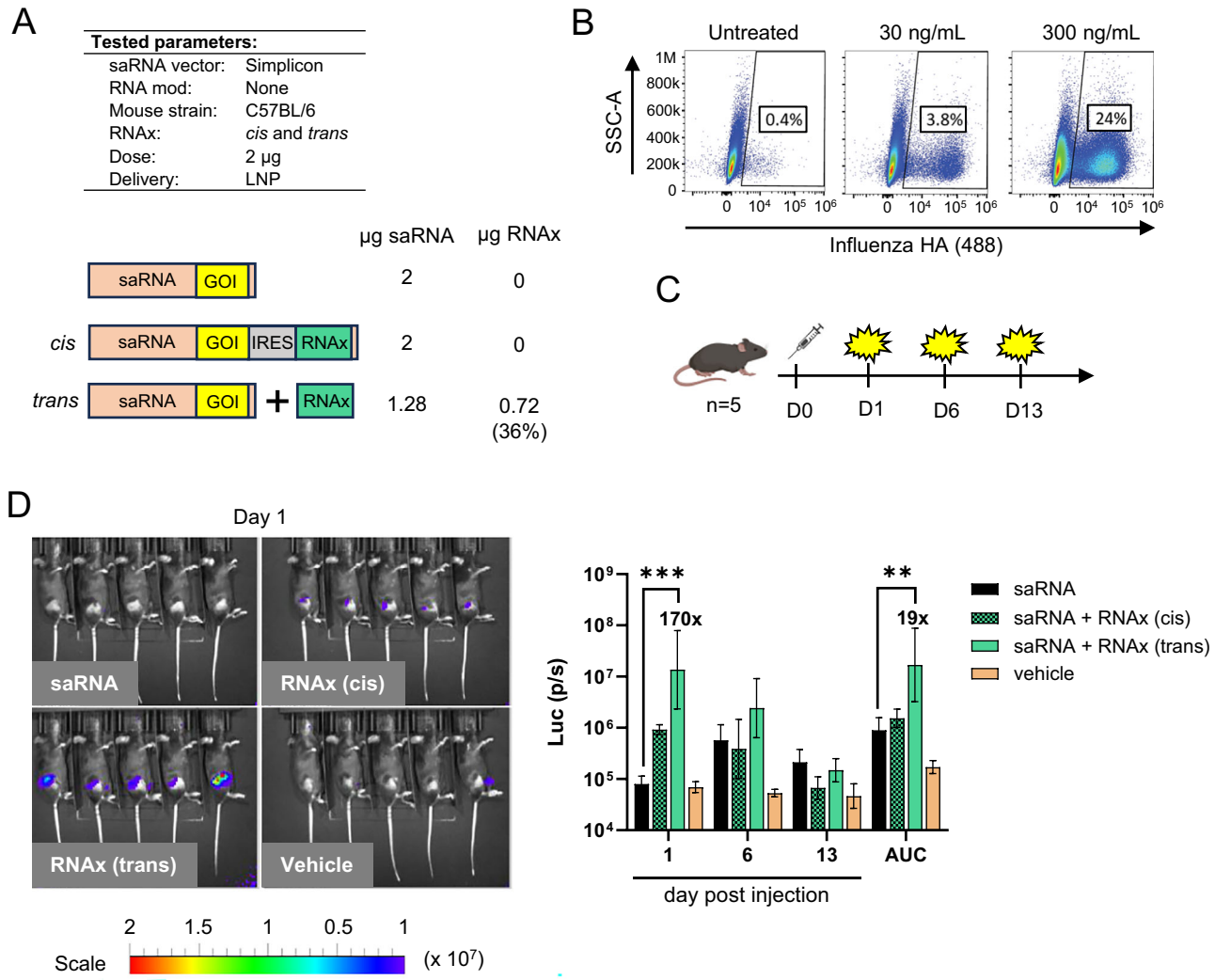

Fig. 2 | RNAx enhances GOI expression from saRNA in vivo. A Unmodified Influenza HA-nLuc expressing saRNA was co-formulated with modified nucleoside RNAx mRNA (in trans) or co-expressed downstream of an IRES (in cis) and packaged into LNPs. 'In trans' co-formulations consisted of at 36% (weight/weight) RNAx mRNA and 64% saRNA i.e., 0.72 µg of RNAx and 1.28 µg saRNA. **B** Flow cytometry of Influenza HA surface expression in 293 T cells treated for 24 h with HA-nLuc saRNA-LNPs (no RNAx) at the indicated concentrations. **C** C57BL/6 mice ($n = 5$ per group) were intramuscularly injected with 2 µg Influenza HA-nLuc expressing saRNA-LNPs and nLuc activity at the injection site quantified with IVIS on the indicated days post injection. **D** Total flux of Luc signal is represented by photons per sec (p/s). Quantification of nLuc activity at the injection site quantified with IVIS on the indicated days post injection or the area under the curve (AUC). Geometric mean ± Geometric SD, $^{**}p < 0.01$, $^{***}p < 0.001$, Kruskal-Wallis test with Dunn's multiple comparisons. Numbers above bars indicate average fold change enhancement of RNAx containing groups relative to saRNA only. Created with BioRender.com.

in trans from a discrete mRNA, sec-nLuc expression was enhanced up to 11-fold in a dose dependent manner (Fig. 1D). To isolate the components of RNA and innate signaling, we also transfected BJ cells with a nucleoside modified fLuc-encoding mRNA and treated cells with recombinant interferon-beta (IFN-β) or the dsRNA analog Poly(I:C), each of which suppressed fLuc expression over 10-fold relative to untreated cells (Fig. 1E). When co-transfecting cells with RNAx, fLuc activity increased by 4 to 7-fold in the presence of IFN-β or Poly(I:C), demonstrating that RNAx partially rescues translation in the presence of excessive innate signaling (Fig. 1E). Together, these results show that RNAx increases GOI expression from saRNA and rescues translation in the presence of excessive innate signaling.

To determine whether RNAx enhances GOI expression from saRNA in vivo, we injected C57BL/6 mice intramuscularly with 2 µg of HA-nLuc saRNA-LNPs with or without RNAx *in cis* or in trans and monitored nLuc activity in vivo at days 1, 6, and 13 post injection (Fig. 2A–C). RNAx in trans yielded a statistically significant enhancement of 170-fold more nLuc expression relative to the saRNA alone group one day post injection ($p < 0.001$, Kruskal–Wallis test with Dunn's multiple comparisons) while changes induced by RNAx *in cis* were not statistically significant (Fig. 2D). We also calculated the area under the curve (AUC) for each formulation by adding the nLuc signal across days. This also revealed that only RNAx in trans resulted in a statistically significant enhancement in GOI expression (19-fold, $p < 0.01$, Kruskal–Wallis test with Dunn's multiple comparisons) (Fig. 2D). Interestingly, nLuc expression in the groups receiving RNAx peaked at day 1 post injection while nLuc activity in the saRNA alone group peaked at day 6 (Fig. 2D). This is consistent with observations by others that GOI expression from saRNA[15] and replication-incompetent RNA viruses[39,40] peak in GOI expression at early time points post injection in mouse backgrounds deficient in IFN signaling. To examine whether RNAx could enhance GOI expression from another inflammatory RNA molecule in mice, we also tested whether RNAx modulated GOI expression from unmodified mRNA, an inducer of innate signaling in vivo[20]. RNAx increased GOI expression up to 12-fold 24 h post injection (Supplementary Fig. 1A, B). These results demonstrate that RNAx enhances GOI expression from multiple forms of inflammatory RNA in vivo.

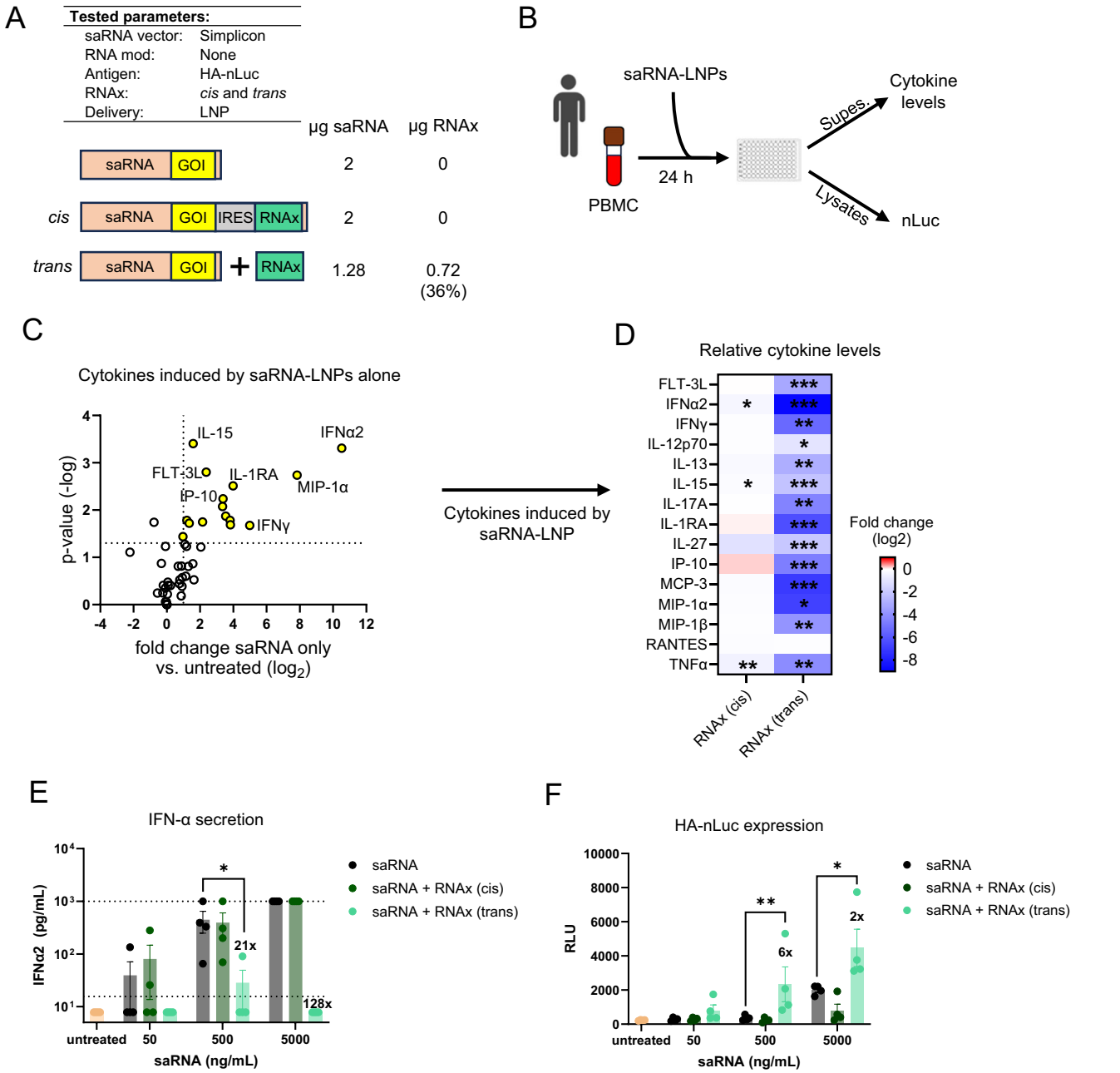

Fig. 3 | RNAx suppresses the expression of proinflammatory cytokines and enhances GOI expression in human PBMC. A Unmodified Influenza HA-nLuc expressing saRNA was co-formulated with modified nucleoside RNAx mRNA (in trans) or co-expressed downstream of an IRES (in cis) and packaged into LNPs. 'In trans' co-formulations consisted of at 36% (weight/weight) RNAx mRNA and 64% saRNA i.e., 0.72 µg of RNAx and 1.28 µg saRNA. **B** Human PBMC ($n = 4$ donors) were treated with HA-nLuc saRNA-LNPs for 24 h and supernatants harvested for cytokines and cell lysates for nLuc activity. **C** The induction of 48 cytokines was measured from supernatants of PBMC treated with 5 µg/mL saRNA-LNPs. Cytokines induced by saRNA alone were determined by comparing the relative levels (ratio of geometric means) between saRNA without RNAx and untreated PBMC. Dotted lines = $p < 0.05$ (ratio paired t-test) and fold change = 2. **D** Among saRNA-LNP-responsive cytokines, the relative impact (ratio of geometric means) of RNAx in cis or trans with saRNA LNPs was determined with the ratio paired t-test (*$p < 0.05$, **$p < 0.01$, ***$p < 0.001$). **E** Supernatants from the same experiment were independently analyzed for IFN-α by ELISA and **F** lysates for nLuc activity. Mean ± SEM, $n = 4$. donors, *$p < 0.05$, **$p < 0.01$ Ratio paired t-test. Dotted lines = upper or lower limit of quantification. Numbers above bars indicate average fold change enhancement or inhibition of RNAx containing groups relative to saRNA only. Created with BioRender.com.

RNAx suppresses proinflammatory cytokines in primary human immune cells

Within its natural viral context, the Cardiovirus leader protein suppresses innate signaling pathways and IFN production[27,28]. We next quantified the impact of RNAx on the induction of proinflammatory cytokines and corresponding GOI expression from saRNA in primary human cells. We treated human peripheral blood mononuclear cells (PBMCs) with HA-nLuc saRNA-LNPs, using the same saRNA-LNPs as tested in Fig. 2A, and quantified the levels of 48 cytokines in the supernatants with a multiplex assay alongside GOI expression from lysates (Fig. 3A, B). We first determined which cytokines were induced by HA-nLuc saRNA-LNPs without RNAx. saRNA alone induced a total of 15 cytokines by at least 2-fold relative to untreated cells ($p < 0.05$, paired t-test), including IFN-α, IFN-γ, and IP-10 (Fig. 3C). With the inclusion of RNAx *in cis* or 36% (w/w) RNAx in trans with HA-nLuc saRNA into LNPs, 14/15 of the saRNA-LNP-induced cytokines were suppressed at least 2-fold ($p < 0.05$, paired t-

test) with RNAx in trans vs. 3/15 with RNAx *in cis* (Fig. 3D, Supplementary Fig. 2D).

We next verified the levels of IFN-α secretion from the same experimental samples with an ELISA and observed potent suppression with RNAx in trans but not *in cis* (Fig. 3E). We also observed a 2- to 6-fold enhancement of nLuc expression by RNAx in trans compared to saRNA alone but not *in cis* (Fig. 3F). To verify the specificity of RNAx-dependent suppression of IFN production based on its known mechanism of action, we used a zinc-finger domain mutant of RNAx, reported to completely inactivate the leader protein of Cardioviruses in general[27]. The zinc-finger mutant protein was unable to suppress the production of IFN-β in BJ cells treated with these HA-nLuc saRNA-LNPs (Supplementary Fig. 2A–C). To estimate transcription factors whose pathway activity may be inhibited by RNAx, we utilized the TRRUST tool, a curated database of transcription factor targets[41]. A broad panel of transcription factors were linked to RNAx (in trans)-sensitive cytokines, including NF-κB, IRF-1/7, and STAT-1/3 (Supplementary Fig. 2E), supporting a model where RNAx suppresses multiple independent signaling pathways.

RNAx suppresses serum biomarkers of reactogenicity from a 5mC-modified Influenza HA saRNA-LNP vaccine

To test the hypothesis that RNAx suppresses proinflammatory cytokines linked to vaccine reactogenicity[42–44] we designed a refined Influenza HA vaccine construct. During the course of our studies, three manuscripts became public which uncovered that 5mC was a suitable modified nucleoside for saRNA vaccines[23,24,45]. Based on these findings, in these experiments we incorporated 5-methylcytidine (5mC) modified nucleosides into the TC-83 strain of VEEV with a construct that expresses only Influenza HA. This construct robustly expressed HA in both 293 T (Fig. 4B) and BJ cells (Supplementary Fig. 3A) and when co-formulated with RNAx (Fig. 4A), displayed enhanced HA expression in BJ cells with RNAx in trans but not *in cis* (Supplementary Fig. 3B). Consistent with the suppression of primary IFN (IFN-α) in PBMCs (Fig. 3E), RNAx in trans also suppressed the secretion of IFN-β and the expression of tetherin, a well-studied IFN-stimulated gene[46] relative to HA saRNA alone in BJ cells (Supplementary Fig. 3C–E). Further supporting a link between innate signaling activation and GOI expression, saRNA did not induce IFN-β secretion or tetherin expression in 293 T cells, alongside a lack of enhanced GOI expression from RNAx (Supplementary Fig. 3B–E). In contrast to RNAx in trans, RNAx *in cis* yielded mixed results: IFN-β levels were potently suppressed (Supplementary Fig. 3C) while tetherin levels were not affected (Supplementary Fig. 3E). Despite robust enhancements of multiple reporter proteins in BJ cells when delivering RNAx *in cis* with a Mirus transfection, in the context of LNP delivery, we observed more consistent and robust GOI expression enhancements with RNAx in trans in human PBMC (Fig. 3F), BJ cells (Supplementary Fig. 3B), and in vivo (Fig. 2D). We also observed more robust and consistent suppression of proinflammatory cytokines across in vitro model systems (Fig. 3D, E, Supplementary Fig. 3E). Based on these data, we focused our studies on RNAx in trans.

C57BL/6 mice were vaccinated with 0.5 μg of 5mC-modified HA saRNA-LNP constructs (Fig. 4A, B) at days 1 and 28 and serum was collected 6 h after each injection (Fig. 4C). We quantified the levels of 18 proinflammatory cytokines with a multiplex assay and IFN-α with an ELISA. First, changes in cytokine levels between vehicle (10% sucrose in Tris-buffered saline pH 7.4) and saRNA alone groups were determined to understand which cytokines were induced by saRNA-LNPs ($p < 0.05$, Mann–Whitney test) (Fig. 4D, G). From those, a follow up test between saRNA alone and different co-formulated amounts of RNAx was conducted to determine the impact of RNAx on saRNA-LNP-induced cytokines ($p < 0.05$ from a Kruskal-Wallis test with Dunn's multiple comparisons) (Fig. 4E, H). A compilation of these data are included in Supplementary Fig. 4.

Following the prime, RNAx suppressed the levels of IFN-α (27-fold), IL-6 (5-fold), KC (3-fold), MCP-1 (6-fold), and TNF-α (1.4-fold) (Fig. 4E, F, Table 1). Following the boost, RNAx suppressed the same cytokines that were induced by saRNA alone in both the prime and boost, as well as IFN-γ (11-fold) and IL-10 (7-fold) (Fig. 4H, I, Table 1). Similar results were found from a different vaccination study with the same HA saRNA-LNPs administered to BALB/c mice (Table 1, Supplementary Fig. 5) as well as an HA saRNA-LNP formulation that utilized an unmodified version of the Simplicon vector that was used in earlier in vitro studies (Table 1, Supplementary Fig. 6). We also examined serum cytokines following injection of unmodified mRNA-LNPs (Supplementary Fig. 1A). RNAx suppressed the levels of IFN-α (22-fold), IL-6 (5-fold), KC (3-fold), and MCP-1 (5-fold) (Supplementary Fig. 1C, D, Table 1). In nearly all cases with each RNA platform (mRNA vs. saRNA) and each saRNA vector (Simplicon vs. TC-83), groups with at least 8% RNAx showed statistically significant inhibition of cytokine levels (Supplementary Figs. 1C, D, 4A, B, 5B–E, 6C–F). Across all saRNA studies IFN-γ, IL-6, KC, MCP-1, and TNF-α were induced by saRNA and suppressed in most cases following the prime or boost (Table 1), pointing to a robust and consistent suppression of cytokines by RNAx that correlate with vaccine adverse events in humans[42–44].

RNAx does not alter the magnitude or Th1/Th2 balance of the cellular response

Because the cellular response to vaccination is heavily influenced by the accompanying induction of innate signaling[8], we next tested whether the potent suppression of the innate response by RNAx in turn negatively impacted the cellular response to vaccination in two of the studies that examined serum biomarkers of reactogenicity (Fig. 4, Supplementary Fig. 6A, D). C57BL/6 mice were vaccinated at day 1 and 28 with 0.5 μg or 0.05 μg of HA saRNA-LNPs with increasing amounts of co-formulated RNAx in trans (Figs. 4A, 5A). Two weeks post boost, splenocytes were isolated and stimulated with an overlapping pool of HA-derived peptides for quantification of IFN-γ and IL-4 secreting cells by ELISPOT. Among the saRNA alone groups receiving 0.5 μg or 0.05 μg doses, only the 0.5 μg dose group yielded a statistically significant increase in IFN-γ-secreting cells vs. vehicle only ($p = 0.0011$, Kruskal-Wallis test with Dunn's multiple comparisons), whereas IL-4 responses remained unchanged compared to vehicle at both doses. Within all dose groups, the inclusion of RNAx did not alter the number of IFN-γ (Fig. 5B) or IL-4 secreting cells (Fig. 5C). Similar results were obtained when examining splenocytes from mice vaccinated with 0.5 μg of the Simplicon-derived HA saRNA-LNP formulations (Supplementary Figs. 6A, 9A–C). Together, these data show that the overall balance as well as the Th1-biased nature of the cellular response is preserved with the inclusion of RNAx.

RNAx enhances antibody titers after single injection of HA saRNA-LNP vaccine

The induction of IL-6 has been shown to be a potent adjuvant for the antibody response to RNA-LNP vaccines[47]. Given that RNAx potently suppressed IL-6 and other cytokine levels post prime and boost (Table 1), we next measured the impact of RNAx on the antibody response from the same studies that examined serum cytokines (Fig. 4, Supplementary Figs. 5, 6A, D). C57BL/6 mice were vaccinated at day 1 and 28 with 0.5 μg or 0.05 μg of 5mC-modified TC-83 HA saRNA-LNPs co-formulated with 1% or 10% (w/w) RNAx (Figs. 4A, 5A). On day 42, serum was analyzed for anti-HA binding IgG antibodies by ELISA. At the 0.05 μg dose, we observed a statistically significant 7-fold increase in binding antibody titers with 10% RNAx ($p < 0.05$, Kruskal-Wallis test with Dunn's multiple comparisons) (Fig. 5D), while at a 0.5 μg total dose, antibody levels remained constant regardless of the dose of RNAx (Fig. 5D). In contrast, RNAx *in cis* did not affect antibody levels (Supplementary Fig. 7B). In a BALB/c mouse vaccination model utilizing an extended dosing interval[6,48–50], we observed a 3-fold increase ($p < 0.05$, Kruskal-Wallis test with Dunn's multiple comparisons) in binding antibody titers post prime from 1% RNAx at the 0.05 μg total dose, but not the 0.5 μg total dose (Supplementary Fig. 8A, B).

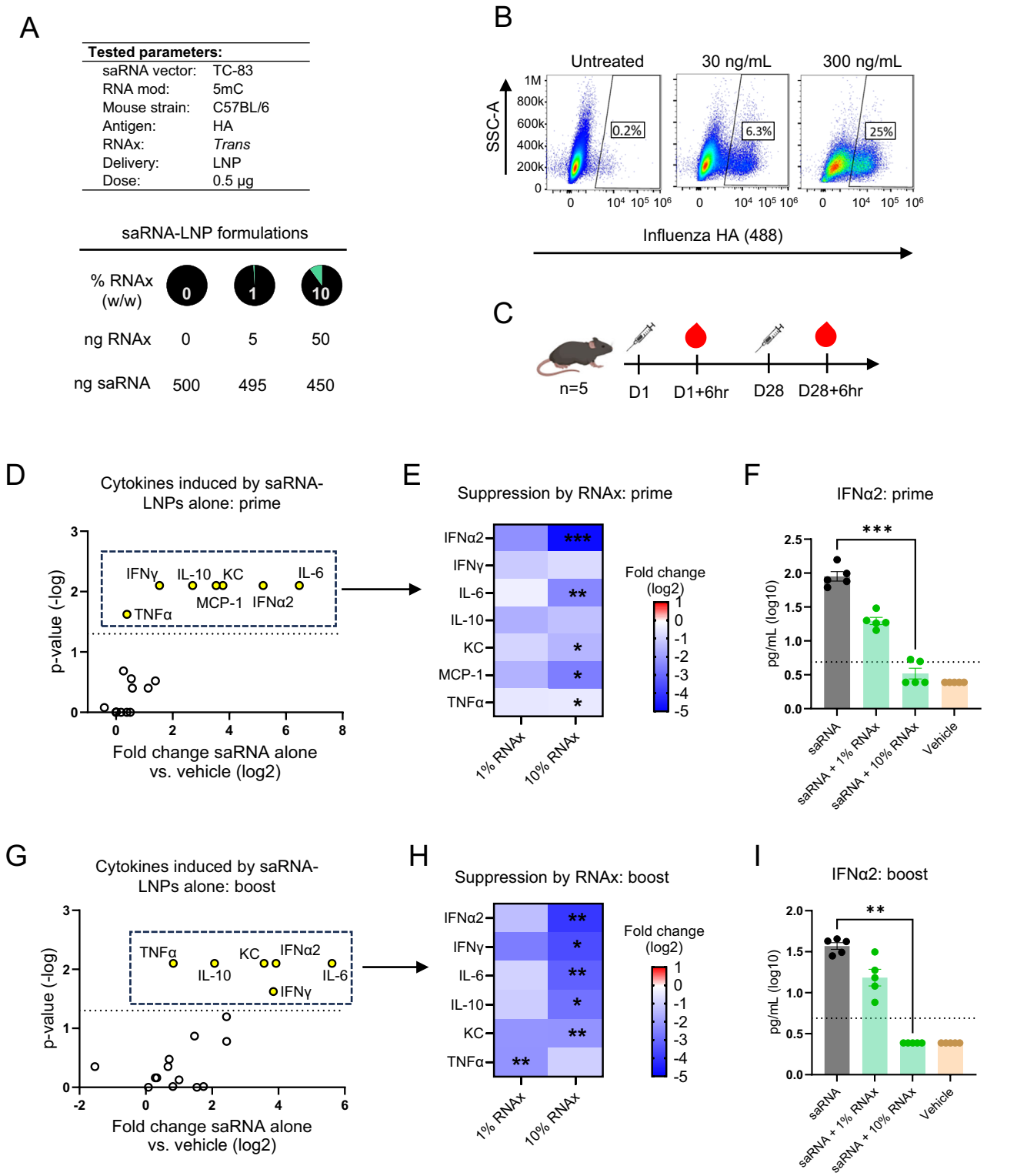

Fig. 4 | RNAx suppresses proinflammatory cytokines in mice following vaccination. **A** 5mC-modified Influenza HA expressing saRNA was co-formulated with modified nucleoside RNAx mRNA in trans at 1% and 10% (weight/weight) into LNPs. **B** Flow cytometry of Influenza HA surface expression in 293 T cells treated for 24 h with HA saRNA-LNPs (no RNAx) at the indicated concentrations. **C** C57BL/6 mice ($n = 5$ per group) were intramuscularly injected with 0.5 µg of Influenza HA saRNA-LNPs and were analyzed for serum cytokines 6 h post injection following (**D**–**F**) the prime on day 1 or (**G**–**I**) the boost on day 28. **D**, **G** Cytokines induced by saRNA only containing LNPs were determined by comparing the relative levels (ratio of geometric means) between saRNA alone and vehicle treated animals. Dotted line = $p < 0.05$ (Mann–Whitney t-test). **E**, **H** Among saRNA-LNP-responsive cytokines, the relative impact (ratio of geometric means) of co-formulating 1% or 10% (w/w) RNAx with saRNA LNPs was determined with Kruskal-Wallis test with Dunn's multiple comparisons (*$p < 0.05$, **$p < 0.01$, ***$p < 0.001$) following the prime and boost, respectively. **F**, **I** Absolute IFN-α abundance levels for all treatment groups following the prime and boost, respectively. Created with BioRender.com.

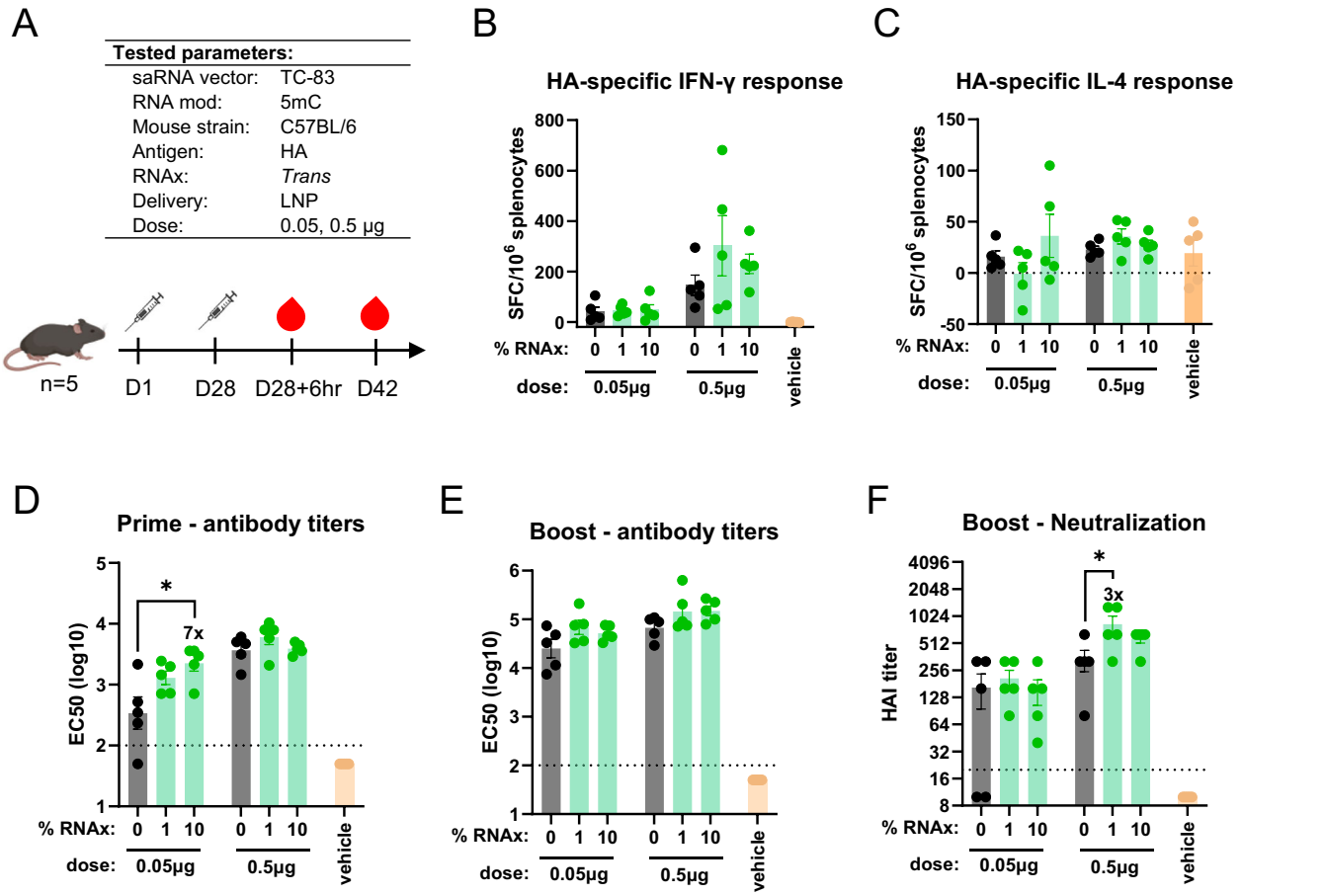

Fig. 5 | Impact of RNAx on immunogenicity from an Influenza HA saRNA-LNP vaccine. A C57BL/6 mice ($n = 5$ per group) were intramuscularly injected (prime and boost) with 0.05 µg or 0.5 µg of HA saRNA-LNPs (see Fig. 4A for details on RNA co-formulations). Serum was collected 6 h after the boost on day 28 (post prime measurement) and serum and splenocytes collected on day 42 (post boost measurement). Splenocytes were treated with 1 µg/mL Influenza HA peptide pools and analyzed for **B** IFN-γ and **C** IL-4 secreting cells by ELISPOT. Spot forming cells (SFC) were subtracted by untreated samples and normalized by 10^6 splenocytes. Mean ± SEM. Total anti-HA IgG in the serum (EC50) was quantified by ELISA at **D** post prime and **E** post boost. **F** Neutralization titers were quantified by HAI assay post boost. Dotted line = lower limit of quantification, Geometric mean ± Geometric SD, $^*p < 0.05$, Kruskal-Wallis test with Dunn's multiple comparisons. Numbers above bars indicate fold enhancement of RNAx containing groups relative to saRNA only. Created with BioRender.com.

We also examined the antibody response in C57BL/6 mice vaccinated with the Simplicon vector HA saRNA-LNP constructs (Supplementary Figs. 6A, 9A) and found that the 2% RNAx group showed a statistically significant ($p < 0.05$, Kruskal-Wallis test with Dunn's multiple comparisons) 7-fold enhancement, while titers from groups with higher amounts of RNAx returned to levels of the control saRNA group (Supplementary Fig. 9D). While the optimal % of RNAx in the formulation for enhancing antibody titers varied across mouse strains and VEEV vectors, in no condition tested did RNAx suppress the antibody response.

RNAx preserves and occasionally enhances the antibody response after vaccine boost

Each of the three vaccination studies were also analyzed for the presence of binding antibody and viral neutralizing titers (HAI assay) 2 weeks post boost. At the 0.5 µg total dose, C57BL/6 mice vaccinated with the 5mC-modified TC-83 construct resulted in neutralization titers 3-fold higher ($p < 0.05$, Kruskal-Wallis test with Dunn's multiple comparisons) with 1% RNAx (Fig. 5F). While binding antibody titers increased 2-fold with this group, this difference was not statistically significant (Fig. 5E). In contrast, RNAx *in cis* did not affect binding or neutralization antibody levels (Supplementary Fig. 7C, D). In the BALB/c vaccination model, mice vaccinated with a 0.05 µg dose, a dose with equivalent binding titers as 0.5 µg vaccinated C57BL/6 mice, showed higher anti-HA antibody binding titers 2-fold in a statistically significant manner with 1% RNAx ($p < 0.05$, Kruskal-Wallis test with Dunn's multiple comparisons) (Supplementary Fig. 8C). Neutralization titers in BALB/c mice receiving 1% RNAx at the 0.05 µg total dose increased slightly but failed to reach statistical significance ($p = 0.067$, Kruskal-Wallis test with Dunn's multiple comparisons) (Supplementary Fig. 8D). In the unmodified Simplicon vector vaccination study (Supplementary Fig. 9A), all of the groups containing RNAx did not significantly change relative to saRNA only following the boost (Supplementary Fig. 9E, F). As with the antibody response following the prime, RNAx amounts that yielded enhancements to the antibody response varied across mouse strains and VEEV vectors. In no condition tested did RNAx *in cis* enhance the antibody response (Supplementary Fig. 7), which combined with the added flexibility of providing RNAx from a separate mRNA makes in trans an attractive means of delivery RNAx. Even at high doses of RNAx in trans, binding antibody and neutralization titers were preserved despite potent suppression of serum biomarkers of innate signaling (Table 1).

Discussion

Optimal immunogenicity is a fine balance between innate signaling and antigen expression[8]. Intuitively, one would expect that suppressing innate signaling-driven reactogenicity would also reduce immunogenicity. Our results cumulatively show that by incorporating RNAx into saRNA vaccines of various backbones and nucleotide modifications, serum biomarkers of vaccine reactogenicity are greatly reduced, in many cases close to the baseline. Despite suppressing innate signaling and reactogenicity

parameters that correlate with traditional avenues of adjuvancy, RNAx did not negatively affect immunogenicity. In fact, in certain conditions, RNAx enhanced the antibody response. We propose that this is due to suppression and not elimination of all necessary innate signaling in conjunction with a corresponding increase in antigen expression. In addition, RNAx suppressed the levels of IFN-α and MCP-1, molecules linked to pathways that can suppress immunogenicity[15,51,52]. This suggests that RNAx can be used to control RNA vaccine side effects while preserving the immune response or enable dose sparing via increased per μg potency.

Each of the model systems we deployed have unique strengths and differences. Early in vitro experiments employed a lipoplex reagent for transfection which appeared to show stronger enhancements from RNAx when delivered *in cis* vs. in trans. However, additional in vitro and in vivo GOI experiments using LNPs for transfection revealed that RNAx in trans was indeed superior, which was also consistent with antibody data following vaccination in mice. We believe that the initial promising results with RNAx *in cis* is at least partially due to the nature of a lipoplex reagent vs. LNPs. Lipoplexes are thought to be much larger than LNPs and may deliver many more copies of RNAx when *in cis* per cell per uptake event, perhaps explaining why RNAx *in cis* initially appeared to be superior in vitro. Subsequent GOI experiments in vitro and in vivo, cytokine release data in PMBC, as well as immunogenicity data in mice demonstrate that in our constructs, RNAx in trans was superior. We suspect that RNAx in trans expresses RNAx to a sufficiently high level, more rapidly, and in more cells than when delivered *in cis*, which may be needed to better counteract the innate signaling pathways that suppress GOI expression. We also observed differences in the optimal dose of RNAx across model systems. For example, while 1% and not 10% RNAx enhanced GOI expression from LNPs in BJ cells, 35% RNAx showed potent enhancements in PBMCs and in vivo. In contrast to in vitro experiments with BJ cells, 10%, but not 1% showed the most striking reduction in serum biomarkers of reactogenicity in vivo. This may be due to differences in transfection efficiency where cells in vivo require a higher total dose of RNAx and underscores the importance of testing human PBMC when possible. The fact that different amounts of RNAx may be optimal in different contexts should facilitate more robust pre-clinical testing from the de-coupling of RNAx dose from saRNA vaccine dose. At lower doses of RNAx that did not potently suppress serum proinflammatory cytokines, we tended to detect enhancements to the antibody response. This suggests that one could also either improve the tolerability of an already highly potent saRNA-LNP vaccine or increase the per μg potency, thereby facilitating dose sparing.

Reducing saRNA-induced innate signaling is an active area of research for improving patient tolerability. One approach has been to incorporate modified nucleotides into the saRNA molecule. Relative to unmodified nucleosides, modified nucleoside-containing saRNA-LNP vaccines have been shown to reduced serum levels of IFNα 2.4-fold in mice[23] and may be associated with lower incidence of systemic adverse events in the clinic[45]. RNAx builds upon these results by further suppressing IFNα levels to below the limit of quantification in our assays, as well as potently reducing levels of IFN-γ, IL-6, MCP-1, and TNF-α. We hypothesize that RNAx-dependent suppression of these cytokines will improve saRNA-LNP vaccine tolerability. In humans, serum levels of IFN-γ, IL-6 and MCP-1 correlated with systemic symptoms following boost with BNT162b2[42] while in the context of an adjuvanted hepatitis B virus vaccine, IFN-γ and IL-6 correlated with systemic symptoms following boost[43]. In addition, serum levels of TNF-α correlated with injection site soreness following injection with an attenuated Influenza vaccine[44]. Supporting these clinical data, IFN-α[53], IL-6[54], and TNF-α[55] are well known to induce flu-like symptoms when administered systemically in humans. While there is a paucity of clinical data quantifying the association of serum biomarkers with saRNA-LNP vaccine tolerability and immunogenicity, future clinical studies deploying RNAx could directly address this question.

While we obtained evidence of RNAx enhancing the antibody response in some contexts, mice are well-known to underestimate the positive effects on vaccine immunogenicity when modulating innate signaling from RNA-LNPs. Nucleoside modifications[19,20] were instrumental in enabling the first clinically approved SARS-CoV-2 mRNA-LNP vaccines BNT162b2[21] and mRNA-1273[22]; however, an unmodified mRNA-LNP vaccine developed by CureVac (CVnCoV) that failed in the clinic[56] generated similar levels of immunogenicity in mice compared to the modified nucleoside vaccines[57–59]. Bernard and colleagues directly compared modified and unmodified nucleoside versions of an mRNA-LNP vaccine in mice and non-human primates (NHP) and found that mice greatly underestimated the beneficial effects of modified nucleosides[60]. CureVac's next generation unmodified mRNA platform (CV2CoV) was engineered to have more efficient antigen expression, which not only outperformed CVnCoV but also achieved similar immunogenicity with BNT162b2 in NHPs[61]. However, CVnCoV and CV2CoV yielded comparable immunogenicity results in mice[62]. Mirroring our findings that RNAx occasionally enhanced immunogenicity in mice, perturbation of the IFN pathway has been found to either enhance[15] or not impact[12,13,17] the antibody response from saRNA-LNP vaccines in mice. In total, the body of work from RNA-LNP vaccines suggest caution is warranted when interpreting vaccine improvements that dampen innate signaling based solely on mouse immunogenicity studies. We propose a holistic approach that incorporates mechanistic studies both in primary human cells as well as mice. Future studies in larger animals or humans are ideally suited to uncover the true impact of RNAx on vaccine immunogenicity.

Co-delivering RNAx in trans is an innovative approach to balance saRNA-driven innate signaling by virtue of being broadly acting, modular, and tunable. There is growing evidence that saRNA platforms activate excessive innate signaling[7] and taming this activation is an active area of research[12,13,17,18,23–26]. One approach has been to co-express inhibitors of innate signaling pathways *in cis*. Co-delivering the MERS ORF4a protein *in cis*, a suppressor of IFN production and PKR activation[63], enhanced antibody titers in rabbits but not mice from a Rabies virus vaccine[12]. Inclusion of the Vaccinia virus proteins 'EKB', inhibitors of the IFN pathway and PKR activation, in trans was shown to enhance GOI expression in vitro and in vivo[26], but any effect on immunogenicity has not been made public to our knowledge. RNAx is distinct from these approaches in that it acts broadly by targeting NCT, not individual innate signaling pathways. We consistently observed more potent enhancement of GOI expression, suppression of proinflammatory cytokines, and enhancement to the antibody response when RNAx was delivered in trans vs. *in cis*. Deploying RNAx in trans from a discrete mRNA has the additional feature of allowing the fine tuning dose as well as being applicable to any currently existing saRNA vaccine.

We focused our efforts on evaluating the role of RNAx only in the context of LNP-based delivery as a proof of principle. A study by Kimura and colleagues showed that perturbation of the IFN pathway through co-delivery of a primary IFN receptor (IFNAR) blocking antibody reliably enhanced antibody titers of an saRNA vaccine with their lipid inorganic nanoparticle (LION) platform, but not with LNPs[13]. Given its potent suppression of IFN, we hypothesize that RNAx will also enhance the antibody response from next generation delivery platforms such as LION and nanostructured lipid carrier (NLC)[13,64].

There are important manufacturing and immunological considerations for deploying RNAx. On the one hand, we predict RNAx to be a universal new class of adjuvant that improves tolerability and potency in humans for any saRNA. Being a discrete mRNA allows its addition to any pre-existing saRNA before encapsulation into a lipid-based (or other) delivery system. This greatly reduces time and cost relative to cloning RNAx *in cis* into unique saRNA constructs. On the other hand, adding an additional RNA species into a single formulation workstream would likely add additional QC and lot release testing, adding to costs and operational risk. In our animal studies we were only able to test RNAx when pre-mixed with

saRNA molecules before formulation into LNPs. We predict that RNAx will function similarly if co-mixed with saRNA after all RNAs have already been independently encapsulated into LNPs. If pre-encapsulated, RNAx could be added to existing vaccines vials just before administration, as in the case with some adjuvants. This would have the benefit of not requiring changes to pre-existing vaccine release testing and could be applied to many different vaccines. While there is the question of what impact an immune response against RNAx could have on vaccine antigen-directed immune responses, we believe the risk of interference with on-target immune responses is low for several reasons. First, we were unable to raise an anti-RNAx antisera in rabbits for use in detecting RNAx protein in vitro (data not shown), suggesting that the intrinsic immunogenicity of RNAx is low. Second, the fact that saRNA in the clinic is more potent than traditional mRNA suggests that the addition of a large (~2490 amino acids), theoretically highly immunogenic polyprotein, the RNA-dependent RNA-polymerase of saRNA, does not interfere with on-target vaccine immune responses. In addition, Krähling et al. found that adding a second vaccine antigen (Ebola NP) did not affect immunogenicity against Ebola GP from saRNA, further supporting the notion that adding highly immunogenic, non-vaccine antigens in saRNA will not necessarily interfere with on-target vaccine potency[65].

In conclusion, our data demonstrate that co-delivery of RNAx is an effective means of dampening excessive innate signaling driven by saRNA-LNP vaccines without sacrificing immunogenicity. Supported by our data with saRNA and unmodified mRNA, any reactogenic nucleic acid-based therapy should benefit from RNAx. For vaccines, we hypothesize that suppressing saRNA-driven innate signaling would improve tolerability as well as enhance immunogenicity for any saRNA platform or target in clinic.

Methods

Cells

Cells were passaged at 37 °C in 5% CO_2. BJ fibroblasts (ATCC, CRL-2522) and 293 T/17 cells (ATCC, CRL-11268) were passaged in complete DMEM (Gibco 10566-016), containing 10% heat-inactivated FBS (VWR, 89510-186) and 100 U/mL of Penicillin-Streptomycin (Gibco, 72400-047).

Cloning and in vitro transcription of RNA

saRNA constructs encoding nLuc, fLuc, the Influenza HA-nLuc fusion, and Influenza HA were derived from the Simplicon vector (Sigma, SCR724). VEEV sequences were amplified by PCR and cloned using HiFi assembly (NEB, E2621). Secreted nLuc was engineered by fusing the human albumin signal peptide (MKWVTFISLLFLFSSAYS) to the N-terminus of nLuc. Influenza HA amino acid sequence was derived from accession ACP41953.1. The TC-83 strain of VEEV (Accession MZ399798.1) was also cloned to express Influenza HA (ACP41953.1). All saRNA sequences are provided in Supplementary Data.

In vitro transcription (IVT) of nLuc, fLuc, or Influenza HA-nLuc saRNA constructs was conducted in-house. IVT templates were generated using PCR with primers encoding a 30 nt polyA tail. The PCR products were gel purified (Zymo research, D4008), followed by an additional DNA purification (NEB, T1030). IVT reactions (NEB, E2040S) were carried out with natural nucleosides and co-transcriptional capping with CleanCap AU (Trilink, N-7114). RNA was purified with silica membrane spin columns (NEB, T2050) and quantified by NanoDrop. In vitro transcription of the Influenza HA saRNA construct derived from the Simplicon vector was performed by Aldevron (Fargo, USA) with natural nucleosides and co-transcriptional capping with CleanCap AU (Trilink, N-7114). In vitro transcription of the Influenza HA saRNA construct derived from TC-83 was performed by Trilink (San Diego, USA) using 5-Methylcytosine (5mC) and co-transcriptional capping with CleanCap AU (Trilink, N-7114). N1-Methylpseudouridine-5'-Triphosphate-modified, CleanCap-AG RNAx mRNA as well as the size-matched, noncoding filler mRNA were synthesized by Trilink (San Diego, USA). Unmodified (L-7602) and 5moU-modified (L-7202) fLuc-encoding mRNA was obtained from Trilink (San Diego, USA).

Lipid nanoparticle (LNP) formulations

LNPs were prepared by microfluidic mixing as follows. First, the RNA samples were diluted to a final concentration of 50 µg/mL in 50 mM NaOAc pH 4.5 (Thermo Scientific Chemicals J63669AK) and 150 mM NaCl (Thermo Scientific Chemicals J60434AE). The lipid mix was prepared in 100% ethanol (Fisher BioReagents BP2818100) by diluting ALC-0315 ionizable lipid (Cayman Chemicals 34337), DSPC (Cayman Chemicals 15100), cholesterol (Cayman Chemicals 9003100), and ALC-0159 PEGylated lipid (Cayman Chemicals 34336). For saRNA-LNPs, lipids were used at the molar ratio of 46.3% ALC-0315/9.4% DSPC/43.5% cholesterol/0.8% ALC-0159 at a final total lipid concentration of 8.09 mM. For fLuc mRNA-LNPs, lipids were used at the molar ratio of 46.3% ALC-0315/9.4% DSPC/42.7% cholesterol/1.6% ALC-0159 at a final total lipid concentration of 8.09 mM. Before each mixing reaction, the flow channel of the microfluidic mixing chip was primed by performing a mock mixing reaction using 1X formulation buffer (without cargo) and 100% EtOH (without lipids) in a total volume of 2 mL. RNA and the lipid mix were combined using the Flex-M microfluidic mixing system (Precigenome) using an RNA-to-lipid flow rate ratio (FRR) of 3:1 at the total flow rate (TFR) of 3 mL/min. Immediately after the mixing, the formed LNPs were diluted 10X in 1X Tris-buffered saline pH 7.4 (Fisher BioReagents BP2471-100) and incubated at RT for 1 h. Thereafter, the stabilized LNPs were concentrated to 0.5 mL and washed 2X using Tris-buffered saline pH 7.4 using the Amicon Ultra 10 kDa MWCO centrifugal filter units (EMD Millipore UFC901024). Sucrose (Thermo Scientific Chemicals AC419762500) in Tris-buffered saline pH 7.4 was added to the LNP formulations as a cryoprotectant at the final concentration of 10% before storage at −80 °C. Sample concentration and encapsulation efficiency were determined using the Quant-iT Ribogreen Assay (Invitrogen R11491). LNP Z-average size and polydispersity index (PDI) were measured using dynamic light scattering (Zetasizer, Malvern). A summary of QC measurements for LNP formulations are listed in Supplementary Table 1.

In vitro transfection

BJ cells were seeded into tissue culture treated-white or standard 96-well cell culture plates in complete DMEM and incubated overnight at 37 °C and 5% CO_2. Opti-MEM cell culture media (Gibco, 31985-062) and Mirus TransIT mRNA-transfection reagent (Mirus Bio, MIR 2225) was brought to room temperature. All mixes were prepared under the biosafety cabinet and all surfaces and pipets were cleaned with RNAse Zap prior to handling of RNA. RNA was thawed on ice and kept on ice during the entire procedure. Up to 100 ng per well of RNA was mixed with Mirus transfection reagent according to the manufacturer's instructions. If applicable, transfection complexes were added to cells immediately before adding 100 ng/mL Poly(I:C) (Fisher Scientific, 42-871-0) or 1 ng/mL IFN-β (Fisher Scientific, 84-99I-F010) and incubated at 37 °C and 5% CO_2. nLuc (Promega, N1120) or fLuc (Promega, G7940) activity was measured two to six days post transfection from the lysates (fLuc, HA-nLuc) or supernatants (secreted nLuc) according to the manufacturer's instructions. Plates were then read on the Biotek Synergy LX plate reader for luminescence. IFN-β protein levels were quantified from supernatants by ELISA (R&D Systems, DIFNB0) or Lumit assay (Promega, CS2032C03). Values below the lower limit of quantification (LOQ) were transformed to 0.5*LOQ.

Human PBMC

Cryopreserved human PBMCs were obtained from IQ Biosciences (cat# IQB-PBMC102). Donor characteristics are listed in Supplementary Table 2. Cells were thawed at 37 °C, pelleted, and resuspended in prewarmed RPMI 1640 (Gibco 61870-036) containing heat-inactivated FBS (VWR, 89510-186). 50 µL of 5×10^6 cells/mL were added to V-bottom 96-well plates and mixed with 50 µL of HA-nLuc saRNA-LNPs for a final concentration of 5000 ng/mL, 500 ng/mL, or 50 ng/mL. Untreated and LPS-treated cells (100 pg/mL final, Invitrogen, 00-4976-93) served as controls. 24 h later, cells were spun at 300 g for 5 min and supernatants stored at −80 °C until cytokine measurements. Cell pellets were analyzed for nLuc activity (Promega, N1120) according to manufacturer's instructions. Lysates were

Table 1 | Summary of maximum fold reduction of proinflammatory cytokines by RNAx

Vector	TC-83	TC-83	Simplicon	mRNA	TC-83	TC-83	Simplicon
RNA mod	5mC	5mC	None	None	5mC	5mC	None
Strain	C57BL/6	BALB/c	C57BL/6	C57BL/6	C57BL/6	BALB/c	C57BL/6
IFNα2	27x	20x	7x	22x	15x	28x	11x
IFNγ		11x	41x		11x	15x	
IL-6	5x	9x	14x	5x	9x		4x
IL-10					7x		
KC	3x			3x	4x		3x
MCP-1	6x	7x	5x	5x		6x	
TNFα	1.4x	3x			2x		1.5x

Compilation of results from Fig. 4 and Supplementary Fig. 1, 4–6. Maximum fold change suppression from RNAx at any dose vs. saRNA or mRNA alone is indicated for differences that were statistically significant ($p < 0.05$ Kruskal-Wallis test with Dunn's multiple comparisons). Red shading is proportional to the magnitude of maximum fold change.

transferred to opaque white plates and read on the Biotek Synergy LX plate reader.

Undiluted cell supernatants were analyzed for the presence of 48 human cytokines using the Luminex™ 200 system (Luminex, Austin, TX, USA) by Eve Technologies Corp. (Calgary, Alberta). Forty-eight markers were simultaneously measured in the samples using Eve Technologies' Human Cytokine Panel A 48-Plex Discovery Assay (MilliporeSigma, Burlington, Massachusetts, USA) according to the manufacturer's protocol. The 48-plex consisted of sCD40L, EGF, Eotaxin, FGF-2, FLT-3 Ligand, Fractalkine, G-CSF, GM-CSF, GROα, IFN-α2, IFN-γ, IL-1α, IL-1β, IL-1RA, IL-2, IL-3, IL-4, IL-5, IL-6, IL-7, IL-8, IL-9, IL-10, IL-12(p40), IL-12(p70), IL-13, IL-15, IL-17A, IL-17E/IL-25, IL-17F, IL-18, IL-22, IL-27, IP-10, MCP-1, MCP-3, M-CSF, MDC, MIG/CXCL9, MIP-1α, MIP-1β, PDGF-AA, PDGF-AB/BB, RANTES, TGFα, TNF-α, TNF-β, and VEGF-A. Cytokines were deemed to be induced by saRNA-LNP if the geometric mean levels were 2-fold higher than untreated and $p < 0.05$ by the ratio paired t-test. Cytokines were deemed suppressed by RNAx if the geometric mean levels were 2-fold lower in the RNAx groups relative to saRNA only groups and $p < 0.05$ by the ratio paired t-test. IFN-α2 levels were independently quantified from the same cell supernatants with the LumiKine Xpress hIFNa 2.0 ELISA (InvivoGen luex-hifnav2) according to the manufacturer's instructions. Values below the lower limit of quantification (LOQ) were transformed to 0.5*LOQ. Transcription factor analysis was conducted with TRRUST version 2 (https://www.grnpedia.org/trrust/, accessed Jan 2025)[41]. Cytokines induced by saRNA alone and subsequently suppressed by RNAx were analyzed with default parameters.

Flow cytometry

3×10^5 293 T cells/well and 1×10^5 BJ cells/well were seeded into 12-well plates in complete DMEM overnight at 37 °C and 5% CO_2. LNPs were diluted in prewarmed complete DMEM and incubated with cells for 24 h at 37 °C and 5% CO_2. Supernatants were collected and frozen at −80 °C while cells were treated with trypsin (Gibco, 12605-010) for 1–5 min, rinsed in complete DMEM, washed in PBS(-/-) (Gibco, 14190-136), then transferred to V-bottom 96-well plates. Cells were then incubated with LIVE/DEAD cell dye for 10 min at RT in the dark. Cells were rinsed in FACS buffer (PBS(-/-) + 1% heat inactivated FBS + 0.05% sodium azide) and then incubated with primary antibody for 1 h at 4 °C in the dark. Human anti-Influenza antibody clone FI6V3 (Creative Biolabs, PABL-214) was conjugated with the Zenon human IgG labeling kit according to manufacturer's instructions (Invitrogen, Z25402). Anti-tetherin (CD317)-APC clone RS38E antibody (Biolegend, 348410) was used to stain for tetherin expression. Cells were rinsed twice in FACS buffer then fixed in 1% PFA (Electron Microscopy Sciences, 15714-5) for 1 h at 4 °C. For compensation beads, UltraComp eBeads Plus Compensation Beads (Fisher Sci, 01-333-342) were used for antibody complexes and ARC amine reactive kit (Fisher Sci, 50-112-1496) for LIVE/DEAD dye. Samples were run on the Attune NxT flow cytometer (Thermo Fisher) and analyzed with FlowJo (10.10.0).

Animal studies

Animal studies at Charles River Laboratories (Worcester, MA) were conducted in compliance with CRL IACUC No. I035. Animal studies performed at Labcorp (Denver, PA) were in compliance with the U.S. Department of Agriculture's (USDA) Animal Welfare Act (9 CFR Parts 1, 2, and 3); the Guide for the Care and Use of Laboratory Animals (Institute of Laboratory Animal Resources, National Academy Press, Washington, D.C., 2011); and the National Institutes of Health, Office of Laboratory Animal Welfare. Whenever possible, procedures in these studies were designed to avoid or minimize discomfort, distress, and pain to animals. Studies conducted at Labcorp were conducted in accordance with Labcorp IACUC protocols, Standard Operating Procedures (SOP), Quality Management Systems (QMS), and Quality Principles (QP).

In vivo imaging

In vivo imaging was performed at Charles River Laboratories (CRL, Worcester, MA) using 8–10 week old female C57BL/6 mice obtained from CRL. Mice were housed in Innovive individually ventilated cages kept under positive pressure during the study and acclimated for 2 days prior to injection. Test articles were thawed and stored at 4 °C. Within 30 min of injection, test articles were equilibrated to room temperature. Mice were injected intramuscularly into the right quadricep with 50 µL containing 2 µg of saRNA-LNPs, 5 µg of mRNA-LNPs, or 50 µL of 10% sucrose in Tris-buffered saline pH 7.4 (vehicle). On days 1, 6, and 13 post injection, mice were intraperitoneally injected with 50 µL of reconstituted Nano-Glo in Vivo FFz substrate (Promega, CS320501), and within 2 h, were anesthetized with isoflurane and imaged using the using the Lumina III in vivo imaging system (IVIS) (Perkin-Elmer). Animals were euthanized via CO_2 asphyxiation. Expression of nLuc was quantified as photons per sec (p/s) and data analyzed in Prism 10.4.0 (GraphPad).

Vaccination studies

Immunogenicity and reactogenicity studies were performed at Labcorp (Denver, PA). 10–12 week old female C57BL/6 or BALB/c mice obtained from CRL. Test articles were thawed and stored at 4 °C. Within 30 min of injection, test articles were equilibrated to room temperature. Mice were injected intramuscularly into the right quadricep with 50 µL containing 2 µg, 0.5 µg, or 0.05 µg of saRNA-LNPs or 50 µL of 10% sucrose in Tris-

buffered saline pH 7.4 (vehicle) at the indicated days per study. Mice were bled retro-orbitally following topical application of proparacaine and blood processed into serum. Samples from animal studies examining immunogenicity read outs were also used for reactogenicity (serum cytokine) measurements. At the completion of each study, animals were euthanized by CO_2 followed by exsanguination.

In vivo cytokine measurements

Serum was diluted 1:2 or 1:6 in PBS and analyzed for cytokine, chemokine and growth factor protein levels using the Luminex 200 system (Luminex, Austin, TX, USA) at Eve technologies Corp. (Calgary, Alberta). Samples from animals injected (primed) with 2 µg of the Simplicon saRNA vector were analyzed for the presence of ten markers using Eve Technologies' Mouse Focused 10-Plex Discovery Assay (MilliporeSigma, Burlington, Massachusetts, USA) according to the manufacturer's protocol. The 10-plex consisted of GM-CSF, IFNγ, IL-1β, IL-2, IL-4, IL-6, IL-10, IL-12p70, MCP-1, and TNFα. All remaining in vivo samples were analyzed for the presence of eighteen markers using Eve Technologies' Mouse High Sensitivity 18-Plex Discovery Assay (MilliporeSigma, Burlington, Massachusetts, USA) according to the manufacturer's protocol. The 18-plex consisted of GM-CSF, IFNγ, IL-1α, IL-1β, IL-2, IL-4, IL-5, IL-6, IL-7, IL-10, IL-12(p70), IL-13, IL-17A, KC/CXCL1, LIX, MCP-1, MIP-2 and TNFα. IFN-α2 levels were quantified with the LumiKine Xpress hIFNa 2.0 ELISA (InvivoGen luex-hifnav2) according to the manufacturer's instructions. Values below the lower limit of quantification (LOQ) were transformed to 0.5*LOQ. Histograms show geometric means, with differences in abundance from RNAx deemed statistically significant if $p < 0.05$ with the Kruskal-Wallis test with Dunn's multiple comparisons.

Anti-Influenza HA ELISA

96-well plates (Greiner BioOne, 655061) were coated with 1 µg/mL of recombinant Influenza HA antigen (Sino Biological, 11085-V08H-100) in PBS overnight at 4 °C. Plates were washed 3x with wash buffer (PBS-T + 0.05% Tween-20) with a BioTek 405LS plate washer and incubated with EZ Block blocking buffer (ScyTek, EZB999) for 2 h at 37 °C. Plates were then washed 3x with wash buffer and incubated with diluted, heat-inactivated (56 °C for 30 min) mouse serum for 1 h at RT. Samples were run in technical duplicate. Plates were then washed 3x with wash buffer and incubated with a 1:4000 dilution (in EZ block) of Goat Anti-Mouse IgG Fc-HRP secondary (Southern Biotech, 1033-05) for 1 h at RT. Plates were then washed 5x with wash buffer and incubated in pre-warmed (37 °C) BioFx TMB One Component HRP Microwell Substrate (Surmodics, TMBW-1000-01) for 30 min at RT, then BioFx 450 nm Liquid Stop Solution for TMB Microwell Substrate (Surmodics, LSTP-100-01) added to plates and read on the Biotek Synergy LX plate reader at absorbance 450 nm within 5 min. Technical replicate absorbance values were averaged and EC50 curves generated with the log(agonist) vs. response -- Variable slope (four parameters) regression analysis with a top=4 constraint in Prism (Version 10.4.0). Values below the lower limit of quantification (LOQ) were transformed to 0.5*LOQ. Data are presented as geometric mean ± geometric SD and statistical significance deemed if $p < 0.05$ (Kruskal-Wallis test with Dunn's multiple comparisons).

ELISPOT

Spleens were removed aseptically and placed in a sterile 5 mL tube containing 3.5 mL of 4 °C CTL media (CTLT-010, CTL) and stored at 2–8 °C until processing. Within 2 h, spleens and media were transferred to a gentleMACS C tube (130-093-237, Miltenyi Biotec) and placed into the gentleMACS Octo Dissociator (Miltenyi Biotec). Spleens were then homogenized using the program "m_spleen_04_01" and homogenates spun at 300 g for 8 min. Supernatant was removed and red blood cells lysed with ACK lysis buffer (A10492-01, Gibco) for 4 min at RT. Lysis was neutralized with 2 mL of CTL media and cells spun at 300 g for 8 min. Supernatant was gently removed and cells resuspended in 5 mL CTL media + 1% Glutamax (35050-061, Gibco) + 1% penn/strep (Sigma, P4333). Cell suspension was passed through a sterile 70 µm tissue screen and counted.

IFN-γ and IL-4 producing cells were analyzed with the Double Color Enzymatic ELISPOT Assay according to the manufacturer's instructions (ImmunoSpot). 3×10^5 splenocytes per well were stimulated with Influenza HA peptide at 1 µg/mL (PM-INFA-HACal, JPT Peptide Technologies), 1 µg/mL ConA, or untreated in duplicate. Plates were imaged on the CTL Analyzer (Series 6 Universal) and processed with the ImmunoSpot software (Version 7.0.34.0). Counts per well were normalized to counts per 10^6 splenocytes and background subtracted (untreated groups).

HAI assay

Serum was treated with RDE (Accurate Chemical, YCC340122) in saline (Moltox, 51-40S022.052) for 37 °C for 16–22 h. RDE was then inactivated by incubating samples at 56 °C in a water bath for 30 min followed by cooling to RT for 15–30 min. Samples were diluted in PBS for a final serum dilution of 1:10. Whole turkey RBC (TRBC) (Lampire, 7209403) was rinsed in ice cold PBS and resuspended to 0.5% in PBS. Samples were serially diluted in PBS and 25 µL of sample mixed with 25 µL of 8 HAU virus (A/California/07/2009) and incubated at RT for 1 h. 50 µL of 0.5% TRBC was added and incubated at RT for 30 min. HAI titers were calculated as the reciprocal of the highest dilution resulting in 100% inhibition of RBC agglutination compared to the RBC only control. Samples were tested in 2–4 technical replicates. Values below the lower limit of quantification (LOQ) were transformed to 0.5*LOQ

Statistical analyses

Statistical tests were conducted in Prism (Version 10.4.0). Significance between groups from in vitro data was determined from a ratio paired t-test ($p < 0.05$) and for in vivo generated data from either the Mann–Whitney test or Kruskal-Wallis test with Dunn's multiple comparisons ($p < 0.05$) as indicated in each figure legend. Q-values for transcription factor associations with cytokines was generated by the TRRUST tool (https://www.grnpedia.org/trrust/, accessed Jan 2025)[41].

Data Availability

Raw data for all graphs presented in this manuscript have been provided as a Source Data file. saRNA vaccine construct sequences are provided in Supplementary Data.

Received: 12 January 2025; Accepted: 14 April 2025;
Published online: 29 April 2025

References

1. Geall, A. J., Kis, Z. & Ulmer, J. B. Vaccines on demand, part II: future reality. *Expert Opin. Drug Discov.* **18**, 119–127 (2023).
2. Lee, J., Woodruff, M. C., Kim, E. H. & Nam, J.-H. Knife's edge: balancing immunogenicity and reactogenicity in mRNA vaccines. *Exp. Mol. Med.* **55**, 1305–1313 (2023).
3. Kis, Z., Kontoravdi, C., Shattock, R. & Shah, N. Resources, production scales and time required for producing RNA vaccines for the global pandemic demand. *Vaccines* **9**, 3 (2020).
4. Oda, Y. et al. 12-month persistence of immune responses to self-amplifying mRNA COVID-19 vaccines: ARCT-154 versus BNT162b2 vaccine. *Lancet Infect. Dis.* **24**, e729–e731 (2024).
5. Oda, Y. et al. Immunogenicity and safety of a booster dose of a self-amplifying RNA COVID-19 vaccine (ARCT-154) versus BNT162b2 mRNA COVID-19 vaccine: a double-blind, multicentre, randomised, controlled, phase 3, non-inferiority trial. *Lancet Infect. Dis*. **24**, 351–360 (2023)
6. Maine, C. J. et al. Safety and immunogenicity of an optimized self-replicating RNA platform for low dose or single dose vaccine applications: a randomized, open label Phase I study in healthy volunteers. *Nat. Commun.* **16**, 456 (2025).
7. Minnaert, A.-K. et al. Strategies for controlling the innate immune activity of conventional and self-amplifying mRNA therapeutics:

Getting the message across. *Adv. Drug Deliv. Rev.* **176**, 113900–113900 (2021).
8. Pulendran, B., Arunachalam, P. S. & O'Hagan, D. T. Emerging concepts in the science of vaccine adjuvants. *Nat. Rev. Drug Discov.* **20**, 454–475 (2021).
9. Caskey, M. et al. Synthetic double-stranded RNA induces innate immune responses similar to a live viral vaccine in humans. *J. Exp. Med.* **208**, 2357–2366 (2011).
10. Beuckelaer, A. D. et al. Type I interferons interfere with the capacity of mRNA Lipoplex Vaccines to Elicit Cytolytic T cell responses. *Mol. Ther.* **24**, 2012–2020 (2016).
11. Hoecke, L. V. et al. The opposing effect of Type I IFN on the T cell response by non-modified mRNA-Lipoplex Vaccines Is determined by the route of administration. *Mol. Ther. Nucleic Acids* **22**, 373–381 (2020).
12. Blakney, A. K. et al. Innate Inhibiting Proteins Enhance Expression and Immunogenicity of Self-Amplifying RNA. *Mol. Ther.* **29**, 1174–1185 (2021).
13. Kimura, T. et al. A localizing nanocarrier formulation enables multi-target immune responses to multivalent replicating RNA with limited systemic inflammation. *Mol. Ther*. **31**, 2360–2375 (2023).
14. Zhong, Z. et al. Immunogenicity and protection efficacy of a naked self-replicating mRNA-Based Zika Virus Vaccine. *Vaccine***7**, 96 (2019).
15. Pepini, T. et al. Induction of an IFN-mediated antiviral response by a self-amplifying RNA vaccine: implications for vaccine design. *J. Immunol.* **198**, 4012–4024 (2017).
16. Gong, Y. et al. A novel self-amplifying mRNA with decreased cytotoxicity and enhanced protein expression by macrodomain mutations. *Adv. Sci.* **11**, 2402936 (2024).
17. Tregoning, J. S. et al. Formulation, inflammation, and RNA sensing impact the immunogenicity of self-amplifying RNA vaccines. *Mol. Ther. Nucleic Acids* **31**, 29–42 (2023).
18. Bathula, N. V. et al. Delivery vehicle and route of administration influences self-amplifying RNA biodistribution, expression kinetics, and reactogenicity. *J. Control. Release* **374**, 28–38 (2024).
19. Karikó, K., Buckstein, M., Ni, H. & Weissman, D. Suppression of RNA recognition by toll-like receptors: the impact of nucleoside modification and the evolutionary origin of RNA. *Immunity* **23**, 165–175 (2005).
20. Karikó, K. et al. Incorporation of pseudouridine Into mRNA yields superior nonimmunogenic vector with increased translational capacity and biological stability. *Mol. Ther.* **16**, 1833–1840 (2008).
21. Polack, F. P. et al. Safety and efficacy of the BNT162b2 mRNA Covid-19 vaccine. *N. Engl. J. Med.* **383**, 2603–2615 (2020).
22. Baden, L. R. et al. Efficacy and safety of the mRNA-1273 SARS-CoV-2 vaccine. *N. Engl. J. Med.* **384**, 403–416 (2020).
23. McGee, J. E. et al. Complete substitution with modified nucleotides in self-amplifying RNA suppresses the interferon response and increases potency. *Nat. Biotechnol*. 1–7 https://doi.org/10.1038/s41587-024-02306-z (2024).
24. Komori, M. et al. Incorporation of 5 methylcytidine alleviates innate immune response to self-amplifying RNA vaccine. *bioRxiv* 2023.11.01.565056 https://doi.org/10.1101/2023.11.01.565056 (2023).
25. Zhong, Z. et al. Corticosteroids and cellulose purification improve, respectively, the in vivo translation and vaccination efficacy of sa-mRNAs. *Mol. Ther.* **29**, 1370–1381 (2021).
26. Beissert, T. et al. Improvement of in vivo expression of genes delivered by self-amplifying RNA using vaccinia virus immune evasion proteins. *Hum. Gene Ther.* **28**, 1138–1146 (2017).
27. Pesch, V., van, Eyll, O. van & Michiels, T. The leader protein of Theiler's Virus inhibits immediate-early alpha/beta interferon production. *J. Virol.* **75**, 7811–7817 (2001).
28. Stavrou, S., Feng, Z., Lemon, S. M. & Roos, R. P. Different strains of Theiler's murine encephalomyelitis virus antagonize different sites in the Type I interferon pathway. *J. Virol.* **84**, 9181–9189 (2010).
29. Borghese, F., Sorgeloos, F., Cesaro, T. & Michiels, T. The Leader Protein of Theiler's Virus prevents the activation of PKR. *J. Virol.* **93**, e01010–e01019 (2019).
30. Delhaye, S., Pesch, V. van & Michiels, T. The leader protein of Theiler's Virus interferes with nucleocytoplasmic trafficking of cellular proteins. *J. Virol.* **78**, 4357–4362 (2004).
31. Ciomperlik, J. J., Basta, H. A. & Palmenberg, A. C. Three cardiovirus Leader proteins equivalently inhibit four different nucleocytoplasmic trafficking pathways. *Virology* **484**, 194–202 (2015).
32. Porter, F. W., Bochkov, Y. A., Albee, A. J., Wiese, C. & Palmenberg, A. C. A picornavirus protein interacts with Ran-GTPase and disrupts nucleocytoplasmic transport. *Proc. Natl. Acad. Sci. USA* **103**, 12417–12422 (2006).
33. Bacot-Davis, V. R., Ciomperlik, J. J., Basta, H. A., Cornilescu, C. C. & Palmenberg, A. C. Solution structures of mengovirus Leader protein, its phosphorylated derivatives, and in complex with nuclear transport regulatory protein, RanGTPase. *Proc. Natl Acad. Sci.* **111**, 15792–15797 (2014).
34. Kong, W. P., Ghadge, G. D. & Roos, R. P. Involvement of cardiovirus leader in host cell-restricted virus expression. *Proc. Natl. Acad. Sci. USA* **91**, 1796–1800 (1994).
35. Zoll, J., Galama, J. M., Kuppeveld, F. J. van & Melchers, W. J. Mengovirus leader is involved in the inhibition of host cell protein synthesis. *J. Virol.* **70**, 4948–4952 (1996).
36. Yarbrough, M. L., Mata, M. A., Sakthivel, R. & Fontoura, B. M. A. Viral subversion of nucleocytoplasmic trafficking. *Traffic* **15**, 127–140 (2014).
37. Nelson, J. et al. Impact of mRNA chemistry and manufacturing process on innate immune activation. *Sci. Adv.* **6**, eaaz6893 (2020).
38. Thoresen, D. T., Galls, D., Götte, B., Wang, W. & Pyle, A. M. A rapid RIG-I signaling relay mediates efficient antiviral response. *Mol. Cell* **83**, 90–104.e4 (2023).
39. Tseng, J.-C., Zheng, Y., Yee, H., Levy, D. E. & Meruelo, D. Restricted tissue tropism and acquired resistance to Sindbis viral vector expression in the absence of innate and adaptive immunity. *Gene Ther.* **14**, 1166–1174 (2007).
40. Winkelmann, E. R. et al. Intrinsic adjuvanting of a novel single-cycle flavivirus vaccine in the absence of type I interferon receptor signaling. *Vaccine* **30**, 1465–1475 (2012).
41. Han, H. et al. TRRUST v2: an expanded reference database of human and mouse transcriptional regulatory interactions. *Nucleic Acids Res.* **46**, D380–D386 (2018).
42. Takano, T. et al. Distinct immune cell dynamics correlate with the immunogenicity and reactogenicity of SARS-CoV-2 mRNA vaccine. *Cell Rep. Med.* **3**, 100631 (2022).
43. Burny, W. et al. Inflammatory parameters associated with systemic reactogenicity following vaccination with adjuvanted hepatitis B vaccines in humans. *Vaccine* **37**, 2004–2015 (2019).
44. Christian, L. M., Porter, K., Karlsson, E. & Schultz-Cherry, S. Proinflammatory cytokine responses correspond with subjective side effects after influenza virus vaccination. *Vaccine* **33**, 3360–3366 (2015).
45. Aboshi, M. et al. Safety and immunogenicity of VLPCOV-02, a SARS-CoV-2 self-amplifying RNA vaccine with a modified base, 5-methylcytosine. *iScience* **27**, 108964 (2024).
46. Tiwari, R., Torre, J. C., de la, McGavern, D. B. & Nayak, D. Beyond tethering the viral particles: immunomodulatory functions of tetherin (BST-2). *DNA Cell Biol.* **38**, 1170–1177 (2019).
47. Alameh, M.-G. et al. Lipid nanoparticles enhance the efficacy of mRNA and protein subunit vaccines by inducing robust T follicular helper cell and humoral responses. *Immunity* **54**, 2877–2892.e7 (2021).
48. Brazzoli, M. et al. Induction of broad-based immunity and protective efficacy by self-amplifying mRNA vaccines encoding influenza virus hemagglutinin. *J. Virol.* **90**, 332–344 (2016).
49. Garcia-Dominguez, D. et al. Altering the mRNA-1273 dosing interval impacts the kinetics, quality, and magnitude of immune responses in mice. *Front. Immunol.* **13**, 948335 (2022).

50. Lu, B. et al. Impact of extended dosing intervals and Ipsilateral versus contralateral boosting on mRNA vaccine immunogenicity in mice. *Vaccines* **13**, 263 (2025).
51. Palacio, N. et al. Early type I IFN blockade improves the efficacy of viral vaccines. *J. Exp. Med.* **217**, e20191220 (2020).
52. Mitchell, L. A., Henderson, A. J. & Dow, S. W. Suppression of vaccine immunity by inflammatory monocytes. *J. Immunol.* **189**, 5612–5621 (2012).
53. Borden, E. C. & Parkinson, D. A perspective on the clinical effectiveness and tolerance of interferon-alpha. *Semin. Oncol.* **25**, 3–8 (1998).
54. Epstein, F. H., Gabay, C. & Kushner, I. Acute-phase proteins and other systemic responses to inflammation. *N. Engl. J. Med.* **340**, 448–454 (1999).
55. Roberts, N. J., Zhou, S., Diaz, L. A. & Holdhoff, M. Systemic use of tumor necrosis factor alpha as an anticancer agent. *Oncotarget* **2**, 739–751 (2011).
56. Kremsner, P. G. et al. Efficacy and safety of the CVnCoV SARS-CoV-2 mRNA vaccine candidate in ten countries in Europe and Latin America (HERALD): a randomised, observer-blinded, placebo-controlled, phase 2b/3 trial. *Lancet Infect. Dis.* **22**, 329–340 (2022).
57. Rauch, S. et al. mRNA-based SARS-CoV-2 vaccine candidate CVnCoV induces high levels of virus-neutralising antibodies and mediates protection in rodents. *Npj Vaccines* **6**, 57 (2021).
58. Vogel, A. B. et al. BNT162b vaccines protect rhesus macaques from SARS-CoV-2. *Nature* **592**, 283–289 (2021).
59. Corbett, K. S. et al. SARS-CoV-2 mRNA vaccine design enabled by prototype pathogen preparedness. *Nature* **586**, 567–571 (2020).
60. Bernard, M.-C. et al. The impact of nucleoside base modification in mRNA vaccine is influenced by the chemistry of its lipid nanoparticle delivery system. *Mol. Ther. Nucleic Acids* **32**, 794–806 (2023).
61. Gebre, M. S. et al. Optimization of non-coding regions for a non-modified mRNA COVID-19 vaccine. *Nature* **601**, 410–414 (2022).
62. Hoffmann, D. et al. CVnCoV and CV2CoV protect human ACE2 transgenic mice from ancestral B BavPat1 and emerging B.1.351 SARS-CoV-2. *Nat. Commun.* **12**, 4048 (2021).
63. Rabouw, H. H. et al. Middle east respiratory coronavirus accessory protein 4a Inhibits PKR-Mediated antiviral stress responses. *PLoS Pathog.* **12**, e1005982 (2016).
64. Voigt, E. A. et al. A self-amplifying RNA vaccine against COVID-19 with long-term room-temperature stability. *Npj Vaccines* **7**, 136 (2022).
65. Krähling, V. et al. Self-amplifying RNA vaccine protects mice against lethal Ebola virus infection. *Mol. Ther.* https://doi.org/10.1016/j.ymthe.2022.10.011 (2022).

Acknowledgements

We thank Craig Wilen and Jonathan Smith for expert technical advice throughout the study and thoughtful comments during the preparation of this manuscript. We thank Jane Srivastava and the Gladstone Institutes Flow Cytometry core for expert assistance and support. We also knowledge the following funding sources for use of Gladstone Institutes Flow Cytometry core machines: NIH S10 RR028962 and the James B. Pendleton Charitable Trust for use of the Attune. Graphics in figures were created with BioRender.com.

Author contributions

J.A.W., I.M., P.V.M., B.M., K.R.B., and T.F. conceptualized the study. J.A.W., R.M.J., I.M., B.F., P.V.M., P.P.M., and B.M. contributed to the development and generation of reagents and assays. J.A.W., R.M.J., I.M., B.F., P.V.M., P.P.M., and B.M. performed in vitro experiments. J.A.W., R.M.J., and B.F. managed in vivo studies and characterized immunogenicity. All authors were involved in study design and analysis. J.A.W. wrote the manuscript. All authors provided feedback and contributed to manuscript preparation.

Competing interests

The authors declare the following competing interests: All authors currently hold equity in and were employed by ExcepGen Inc. at the time of this study. ExcepGen Inc is an applicant for the following patents, pending in the US and other countries, based on this work. B.M. and T.F. are inventors of WO 2021/055369 for compositions and methods for enhancing protein expression using an NCT inhibitor protein. B.M., T.F., and I.M. are inventors of WO 2022/192694 for compositions and methods for enhancing protein expression using an NCT inhibitor protein. B.M., T.F., and I.M. are inventors of WO 2022/197940 for compositions and methods for vaccines using an NCT inhibitor protein. B.M., T.F., I.M., and J.A.W. are inventors of WO 2023/183889 for compositions and methods for protein expression using RNA encoding an NCT inhibitor protein.

Additional information

Supplementary information The online version contains supplementary material available at https://doi.org/10.1038/s41541-025-01135-8.

Correspondence and requests for materials should be addressed to Jason A. Wojcechowskyj or Thomas Folliard.